

Effect of starting materials on the properties of solid-state reacted barium titanate powder

Hyun-Tae Kim, Jong-Hyun Kim, Won-Sik Jung and Dang-Hyok Yoon*

School of Materials Science and Engineering, Yeungnam University, Gyeongsan 712-749, Korea

This study examined the effects of the combination of starting materials on the properties of solid-state reacted BaTiO₃ using two different types of BaCO₃ and TiO₂. The reaction temperature was evaluated by thermal gravimetry/differential thermal analysis (TG/DTA). In addition, the effect of mechanochemical activation by high energy milling and the Ba/Ti molar ratio on the reaction temperature, particle size and tetragonality were investigated. TG/DTA demonstrated that the TiO₂ phase and size plays a major role in decreasing the reaction temperature and particle size. With the optimum selection of starting materials and processing conditions, BaTiO₃ with a particle size < 200 nm and a tetragonality (= c/a) of approximately 1.008 was obtained.

Key words: BaTiO₃, Solid-state reaction, Particle size, Tetragonality.

Introduction

BaTiO₃ is the main material for the active layers in multilayer ceramic capacitors (MLCCs). The capacitance of MLCC is proportional to the permittivity of the dielectric layers and inversely proportional to the layer thickness. Therefore, recent efforts have focused on enhancing the volumetric efficiency of MLCC by increasing the dielectric constant of the powders and/or decreasing the layer thickness [1]. The dielectric thickness of an MLCC with currently the highest capacitance is < 1 μm, and is expected to be reduced further in the near future. To meet this requirement, BaTiO₃ powders no more than 200 nm in size with a high dielectric constant are needed because 5 grains are essential in each layer to ensure reliability. However, the dielectric constant decreases with decreasing particle size and disappears below a certain particle size due to a tetragonal to cubic phase transition [2]. Hence, many attempts have been made to increase the dielectric constant whilst maintaining a particle size as small as possible. Tetragonality, which is the relative c-to a-axis ratio (= c/a), is used to make an easy estimation of the dielectric constant with a powder form [3]. The crystal structure should have high tetragonality in order to achieve a high dielectric constant [4].

BaTiO₃ is produced conventionally by a solid-state reaction between BaCO₃ and TiO₂ at temperatures higher than 1000 °C, which generally results in agglomeration, poor chemical homogeneity and a coarse particle size [5]. Due to these drawbacks, a variety of wet chemical methods,

such as hydrothermal [6], sol-gel [7] and coprecipitation [8], have been used for mass production despite their high cost. However, the continuous demand for lower priced MLCCs has focused the powder manufacturer's attention to solid-state reaction methods, which have the merits of low production cost and precise stoichiometry control. In this respect, it is important to understand the fundamentals of the solid-state reactions of BaTiO₃ in order to make the powder characteristics similar or even superior to those produced by wet chemical methods.

Since a solid-state reaction occurs at the contact points of the starting materials, the use of very fine BaCO₃ and TiO₂ is very important for enhancing the reaction rate and decreasing the processing temperature. Moreover, efficient milling of the starting materials can decrease the reaction temperature further due to homogeneous mixing and mechanochemical activation, which alters the chemical and physical properties of the raw materials [9]. Fortunately, both nano-sized starting materials and high energy mills for efficient milling are currently available.

This study examined the effects of 4 different starting material combinations using 2 different types of BaCO₃ and TiO₂ on the solid-state reaction temperature and resulting properties of the synthesized BaTiO₃ particles. The mechanochemical effects were also examined using 2 different milling methods: ball milling and high energy milling. In addition, the effects of the Ba/Ti molar ratio on the particle size and tetragonality (= c/a) were investigated for a chosen starting material combination.

Experimental Procedure

Four types of BaTiO₃ were synthesized from combinations of two different types of BaCO₃ and TiO₂. Table 1

*Corresponding author:
Tel : +82-53 810 2561
Fax: +82-53 810 4628
E-mail: dhyoon@ynu.ac.kr

Table 1. Characteristics of the starting materials

Sample	Materials	Supplier	D_m (nm)	BET (m^2/g)
A	Needle-shaped $BaCO_3$	Solvay	237	16.5
B	Spherical $BaCO_3$	Kojundo	845	1.7
C	Anatase- TiO_2	Showa	16	50.0
D	Rutile- TiO_2	Kanto	245	8.5

summarizes the physical properties of the starting materials including the phase of TiO_2 , particle size and specific surface area along with their nomenclature. Fig. 1 shows electron microscope images of the starting materials, indicating the difference in particle size. The two types of $BaCO_3$ were fine needle-shaped (noted as A) and coarse spherical-shaped $BaCO_3$ (B). The TiO_2 was fine anatase (C) and coarse rutile (D).

The $BaCO_3$ and TiO_2 powders were mixed to a Ba/Ti molar ratio of 1/1 for the 4 combinations in water. The mixtures were then ball-milled for 10 hours using 2 mm ZrO_2 balls and dried to a constant weight. Thermogravimetric/differential thermal analysis (TG/DTA: SDT Q600, TA Instruments, USA) was performed on the mixtures in a flowing air atmosphere at a heating rate of $5\text{ K}\cdot\text{minute}^{-1}$. The samples quenched at 700 and 800 °C were analyzed by X-ray diffraction (XRD: RINT 2200, Rigaku using $Cu\ K\alpha$, 40 kV and 40 mA, continuous scan

at $4^\circ/\text{minute}$ with a collection width of 0.02°) to confirm $BaTiO_3$ formation based on the TG/DTA results.

The AC combination showed the most desirable reaction characteristics. Therefore, further experiments were carried out using this combination. In order to evaluate the mechanochemical activation, 400 grams of the AC combination was milled using a high-energy mill (MiniCer, Netzsch, Germany) for 8 hours at a rotor speed of 3,000 rpm with 0.45 mm ZrO_2 beads. In addition, the AC combination was prepared at a Ba/Ti molar ratio of 0.995, 1.000, and 1.005 by 10 hours of ball-milling, followed by heat treatment between 900–1200 °C for 1 hour in air at a heating rate of $5\text{ K}\cdot\text{minute}^{-1}$.

The particle shape, and crystal structure and tetragonality were determined by scanning electron microscopy (SEM: S-4100, Hitachi), transmission electron microscopy (TEM: H-7600, Hitachi) and XRD, respectively. The Ba/Ti molar ratio was confirmed using X-ray fluorescence spectroscopy (XRF: Simultix 12, Rigaku). The average particle size was estimated from the SEM images by measuring the maximum and minimum diameter of 100 particles using image analyzing software (SigmaScan, Systat Software, USA).

Results and Discussion

Fig. 2 shows the TG/DTA results for the starting material combinations. All samples showed a total weight loss

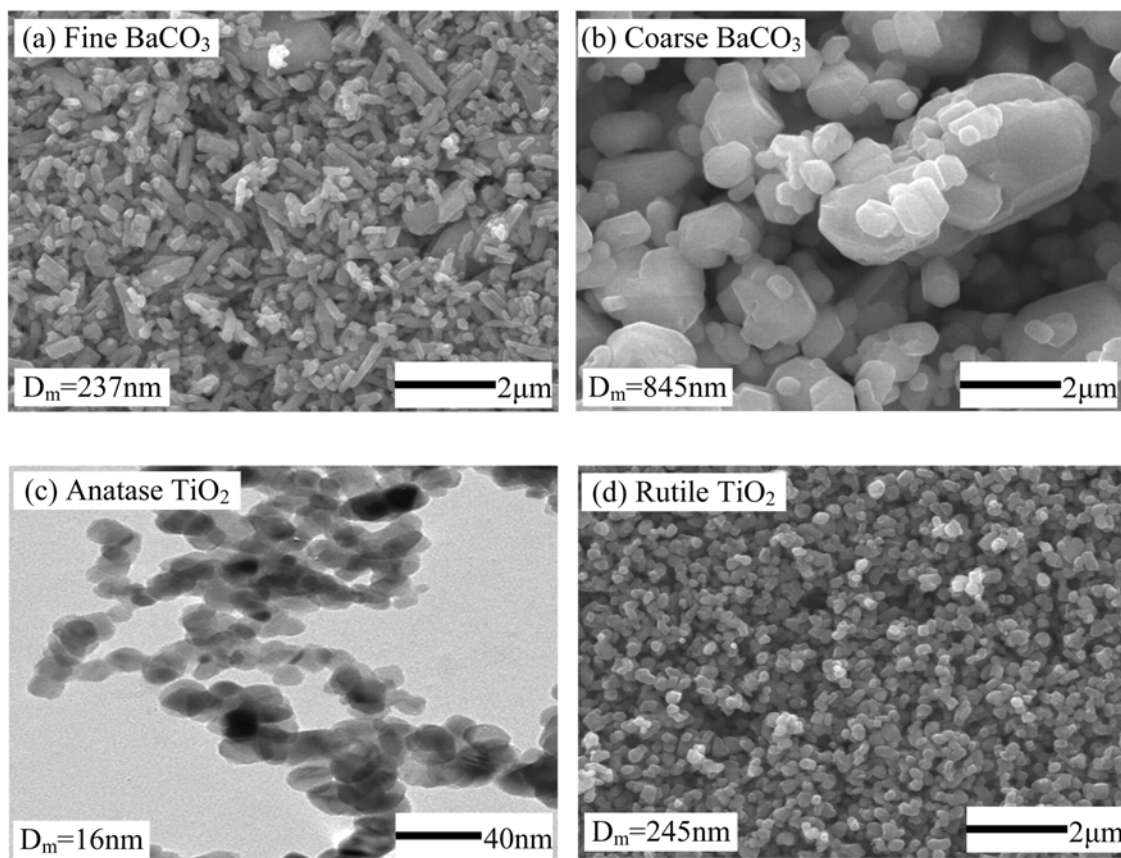


Fig. 1. Electron microscope images of the starting materials: (a) fine and (b) coarse $BaCO_3$, and (c) anatase and (d) rutile TiO_2 .

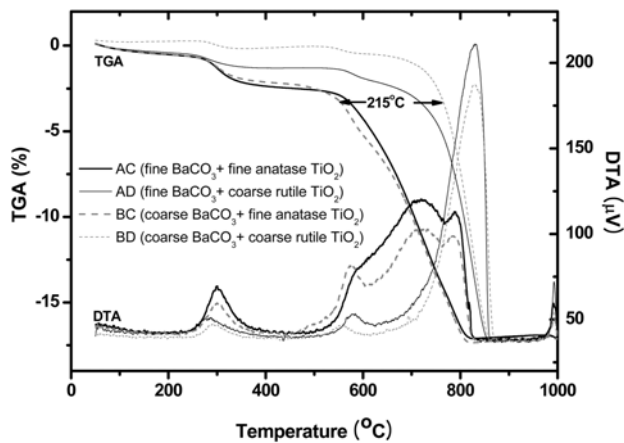


Fig. 2. TG/DTA results for the 4 different combinations of starting materials in air.

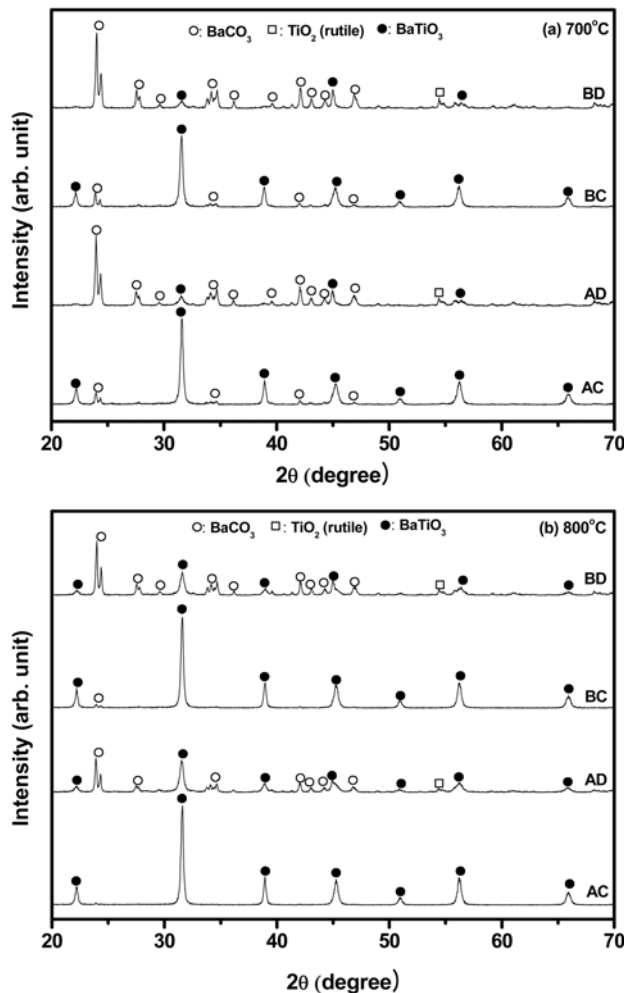


Fig. 3. XRD patterns for the 4 different combinations after quenching from (a) 700 °C and (b) 800 °C.

of approximately 17 wt. %. However, AC and BC with fine anatase TiO_2 exhibited a lower decomposition temperature, where the maximum difference is more than 200 °C as shown in the figure, than AD and BD with coarse rutile

TiO_2 . The exothermic DTA peaks of AC and BC began at a lower temperature and had a broader shape than those of AD and BD. According to the solid-state reaction mechanism proposed by Beauger *et al.* [10], BaCO_3 decomposes into BaO and CO_2 , where TiO_2 acts as a catalyst for this decomposition. TiO_2 never decomposes through a solid-state reaction. Ba^{2+} diffuses into the virgin TiO_2 to form BaTiO_3 . Therefore, fine TiO_2 offers a shorter diffusion length than the coarse one, requiring a faster reaction time. Moreover, Ba^{2+} diffusion into anatase TiO_2 would be easier than that into rutile due to the lower density of anatase (3.90 g/cm³) than rutile (4.23 g/cm³). On the other hand, fine BaCO_3 is more favorable than the coarse BaCO_3 when coarse rutile TiO_2 is used. The difference in decomposition temperature of several tens of degrees Celsius between AD and BD was attributed to the effect of the BaCO_3 particle size, which is smaller than the effect of TiO_2 . Since the solid-state reaction occurs from the interface between dissimilar particles, finer BaCO_3 enhances the reaction rate due to the increased contact points.

Fig. 3 (a) and (b) shows the XRD patterns for the samples quenched from 700 and 800 °C, respectively. Most of the AC and BC starting materials had already transformed into BaTiO_3 with small amounts of BaCO_3 , while only small amounts of BaTiO_3 were formed with the AD and BD starting materials for the 700 °C quenched samples. At 800 °C, all the AC and BC combinations had transformed into BaTiO_3 , while unreacted BaCO_3 and rutile TiO_2 still remained in the AD and BD samples, which is consistent with the TG/DTA results shown in Fig. 2. The XRD pattern shows the simultaneous decomposition of BaCO_3 and the formation of BaTiO_3 .

Fig. 4 shows the SEM morphology of synthesized BaTiO_3 along with the mean particle size and tetragonality after heat treatment at 1000 °C for 1 hour in air. The particles derived from fine anatase TiO_2 were much smaller than those derived from coarse rutile TiO_2 because the size of BaTiO_3 particles is determined primarily by the size of the TiO_2 particles. Although the BC combination shows the smallest particle size of 148 nm, it has a cubic form without any significant peak separation in the XRD pattern between the c- and a-lattice parameter. The MLCC industry prefers to use BaTiO_3 particles <200 nm in size with a tetragonality > 1.008 [11]. The AC combination in this study almost meets these requirements. These criteria are quite difficult to satisfy using wet chemical methods such as hydrothermal and oxalate routes.

Fig. 5 (a) and (b) shows the starting material distribution after 10 hours of ball milling and 8 hours of high energy milling. The coarse needle-shaped BaCO_3 still remains after ball milling, while all the materials were milled into very fine nano-sized particles after high energy milling, highlighting the high milling efficiency. Compared to the conventional ball mills, modern high energy mills equipped with a high speed rotor rotating up to several thousands times per minute are known to be quite effective for milling. Their high energy input and use of small

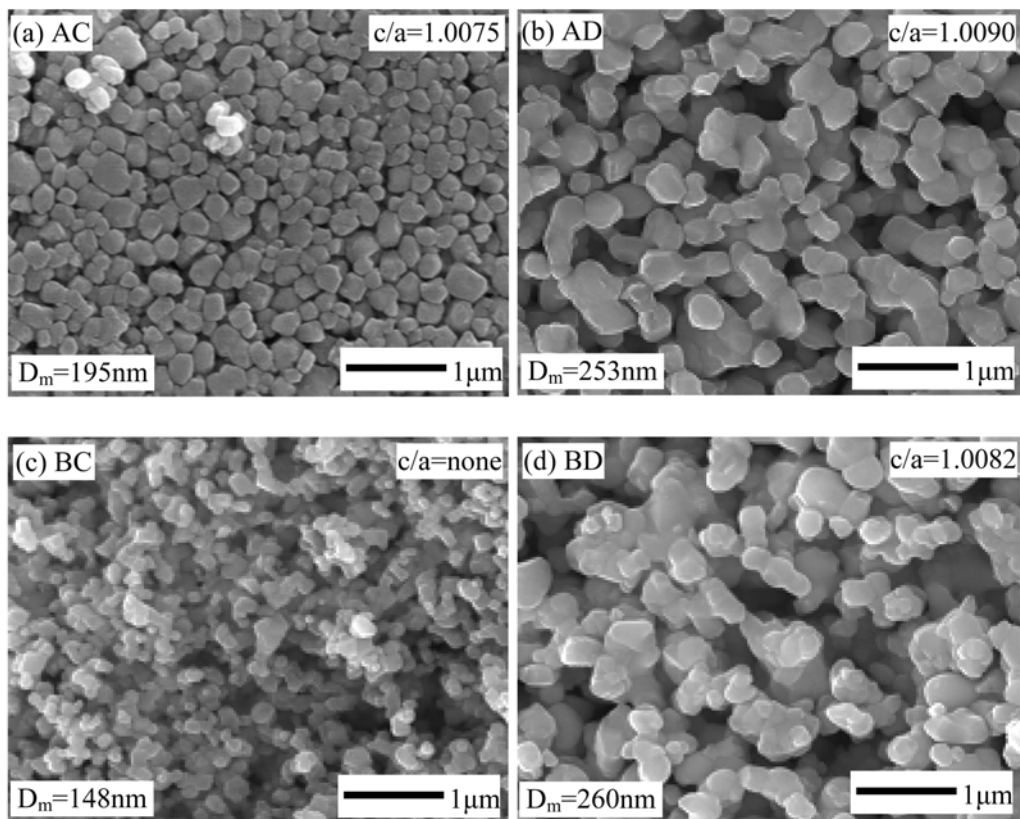


Fig. 4. SEM images of the BaTiO₃ particles synthesized from 4 different combinations by heat treatment at 1000 °C for 1 hour in air. The mean particle size and tetragonality ($=c/a$) are shown.

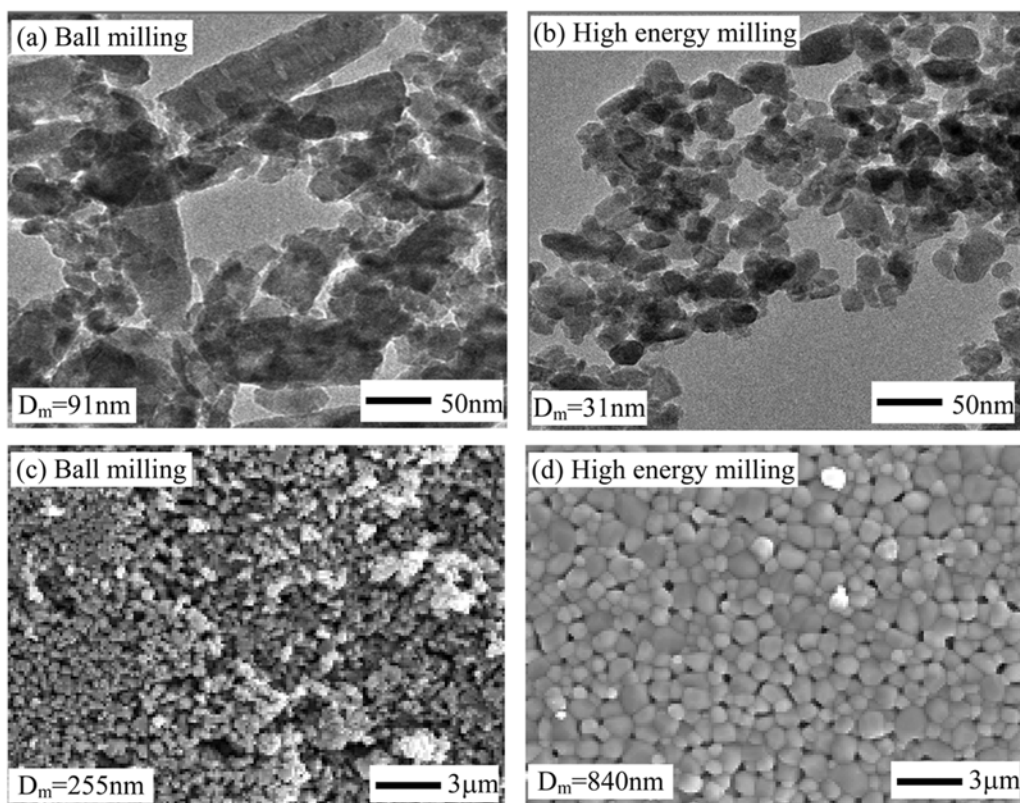


Fig. 5. TEM images of the starting materials after (a) 10 hours of ball milling and (b) 8 hours of high energy milling, and the corresponding SEM images of the synthesized BaTiO₃ particles ((c) and (d), respectively) after heat treatment at 1100 °C for 1 hour.

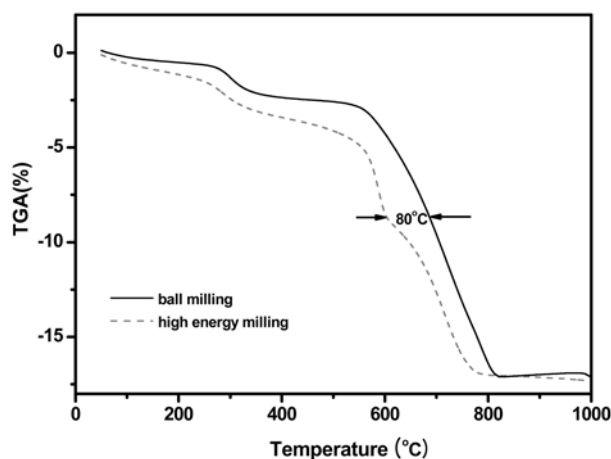


Fig. 6. The TG results of the starting materials after 10 hours of ball milling and 8 hours of high energy milling.

grinding media allow the achievement of a very small particle size in a very short processing time [12]. The mean particle size of the ball-milled powder is 255 nm, while high energy-milled one is 840 nm after heat treatment at 1100 °C. This growth in particle size can be explained by the mechanochemical activation associated with high energy milling. Based on the TG comparison between the ball-milled and high energy-milled starting materials shown in Fig. 6, the reaction temperature can be reduced further by mechanochemical activation of the starting materials.

Fig. 7 shows the relationships between the particle size and tetragonality at 4 different heat treatment temperatures as a function of the Ba/Ti molar ratio (Ba/Ti = 0.995, 1.000 and 1.005). XRF confirmed that the deviation from the target molar ratio $< \pm 0.001$. The particle size decreased with increasing Ba/Ti molar ratio at a fixed temperature. Moreover, the higher tetragonality was easier to achieve at higher Ba/Ti ratios than at low ratios for a similar particle size. Since the X5R or X7R MLCC requires minimum grain

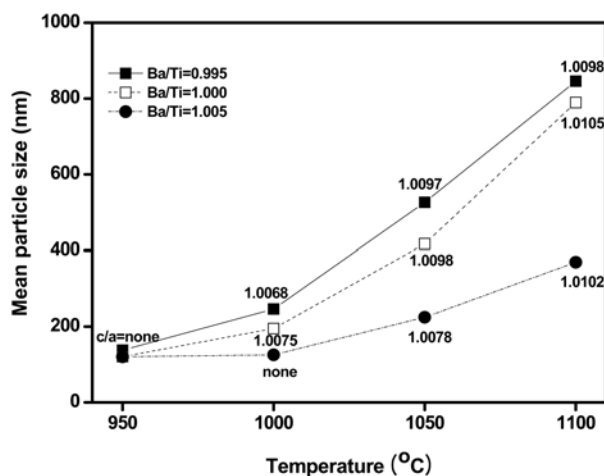


Fig. 7. Relationships between the Ba/Ti molar ratio, particle size and resulting tetragonality as a function of the heat treatment temperature.

growth during sintering and a high dielectric constant, the results shown in Fig. 7 suggest that a BaTiO₃ powder with a slight excess of Ba ions is desirable.

Conclusions

A systematic study on the solid-state reaction of BaTiO₃ was carried out using two different types of BaCO₃ and TiO₂. The following conclusions were obtained:

1. The utilization of fine anatase TiO₂ had a much lower reaction temperature and smaller BaTiO₃ particle size than that of coarse rutile TiO₂ due to the shorter diffusion length and easier diffusion of Ba²⁺ into TiO₂.
2. High energy milling was more efficient than ball milling in terms of mechanochemical activation and milling of the starting materials, and the reaction temperature could be reduced further by this milling process.
3. The solid-state reaction could be completed at temperatures < 800 °C using fine starting materials and mechanochemical activation. The resulting properties of BaTiO₃ were even superior to those formed by wet chemical methods for high capacitance MLCC application.
4. The particle size decreased with increasing Ba/Ti molar ratio of the starting materials at a fixed temperature. On the other hand, higher tetragonality was acquired at higher Ba/Ti ratios for a similar particle size.

Acknowledgements

This study was supported by a Yeungnam University research grant in 2008.

References

1. D.H. Yoon, J. Ceram. Proc. Res. 7[4] (2006) 343-354.
2. K. Uchino, E. Sadanaga and T. Hirose, J. Am. Ceram. Soc. 72 (1989) 1555-1558.
3. S.W. Kwon and D.H. Yoon, J. Eur. Ceram. Soc. 27 (2007) 247-252.
4. T. Tsurumu, T. Sekine, H. Kakemoto, T. Hoshina, S.M. Nam, H. Yasuno and S. Wada, J. Am. Ceram. Soc. 89[4] (2006) 1337-1341.
5. E. Brzozowski and M.S. Castro, Thermochemica Acta 398 (2003) 123-129.
6. Y. Hotta, K. Tsunekawa, T. Isobe, K. Sato and K. Watari, Mater. Sci. Eng. A 475 (2008) 12-16.
7. X. Wang, B.I. Lee, M. Hu, E.A. Payzant and D.A. Blom, J. Eur. Ceram. Soc. 26 (2006) 2319-2326.
8. S. Wada, M. Narahara, T. Hoshina, H. Kakemoto and T. Tsurumi, J. Mater. Sci. 38 (2003) 2655-2660.
9. S. Ohara, A. Kondo, H. Shimoda, K. Sato, H. Abe and M. Naito, Mater. Lett. 62 (2008) 2957-2959.
10. A. Beauger, J.C. Mutin and J.C. Niepce, J. Mater. Sci. 18 (1983) 3041-3047.
11. S.W. Kwon and D.H. Yoon, Ceram. Int. 33 (2007) 1357-1362.
12. N. Darsono, D.H. Yoon and J. Kim, App. Surf. Sci. 254 (2008) 3412-3419.